

Control of Pursuit Eye Movement

M. S. Sugathadasa, W. P. Dayawansa and C. F. Martin

Department of Mathematics

Texas Tech University

Lubbock, TX 79409

Abstract

A dynamic model representing the pursuit eye movement is studied here. It is known that feedback control is used in this type of eye movement. A representative feedback control law is designed and simulations are carried out to demonstrate its effectiveness.

1 Introduction

The eyes move in order to place an intended object on the region of the retina with greatest visual acuity, called the fovea. Movement of eyes are produced via the coordinated action of several muscle groups acting in response to neurological signals. The focus here is to study a particular type of eye movement called smooth pursuit from the perspective of control theory.

There are several types of eye movements reported in the research literature. For example Troost [8] (see also [10, 11, 9, 6, 1] for additional detail) describe four subsystems of the supranuclear ocular motor control (i.e., distinction originates in the higher regions of the brain): (1) saccadic or fast eye movement subsystem, (2) pursuit or tracking subsystem, (3) vergence subsystem, (4) vestibular subsystem. **Saccades** are rapid binocular eye movements which are under both voluntary and reflex control. The visual stimulus for a saccade is the displacement of the target object. Typically saccades occur with a latency of 200 to 250 msec after an instantaneous displacement of the target. Saccades are ballistic (i.e., under open-loop control, and cannot be redirected once the motion is initiated) and the peak velocity can range from $30^0/\text{sec}$ to $700^0/\text{sec}$ with up to 40^0 amplitude. Eye movement during a saccade is relatively simple: an

appropriate latency followed by a period of acceleration to peak velocity followed by deceleration of the eyes onto the new target position. Correspondingly, the control action taken is also relatively simple. The second type, the **pursuit** eye movement, is evoked by the slow movement of a fixated target after a latency of about 125 msec. Maximum eye velocity can go up to $50^0/\text{sec}$. In contrast to saccadic eye movement pursuit eye movement is smooth, and can be continuously modified in response to visual input (i.e., under feedback control). Retinal velocity error is thought to be the input signal to the pursuit control system. This suggestion is corroborated with physiological evidence that demonstrate that pursuit cannot be initiated voluntarily, i.e., without an actual target motion. Attempts to initiate pursuit voluntarily leads to a series of small saccades called the “cog-wheel” pursuit. The third type, the **vestibular-ocular** eye movement, occur as a compensatory response to a head movement, and is elicited by the vestibular system. The latency can be up to 100 msec and the peak eye velocity can be as fast as $300^0/\text{sec}$. In general, the eyes move in an opposite direction to the movement of the head, and the counterrotation, which may match exactly under well lit conditions, takes place as a smooth movement under continuous feedback control interrupted by intermittent saccades that recenter the eyes toward midposition in the orbit. It is thought that the head acceleration is the input signal during the feedback control (i.e., continuous) phase. The fourth type, the **Vergence** eye movement, occur in response to motion toward or away from the observer. The latency is approximately 160 msec and the maximum velocity is about $20^0/\text{sec}$.

There is much biological evidence to suggest that the smooth pursuit eye movement and the saccadic

eye movement are fundamentally different neurological phenomena, among them are the region of origin of control signals in the brain (see e.g. [7]) and the pathways (for example, it is reported in [8] that horizontal saccades originate in the cortex of the contralateral frontal lobe, whereas pursuit originate in the ipsilateral parieto-occipital visual association areas). Differences have been found regarding the other types eye movements as well (see e.g., [8]).

2 Oculomotor Plant Model

There have been many recent studies aimed at modeling the dynamics of the eye movement (see e.g., [2],[3],[4],[5]). A common theme in all this work is to model the eye as a rigid body controlled by muscles attached to it. They differ in the way the muscles are modeled. It is our viewpoint that the nonlinear dynamics of muscles play a central role. In this regard, recent models developed by [2] are the most relevant.

In his M.S. thesis [2], A. McSpadden derived a system of dynamical equations to describe the eye movement in a horizontal plane. Attention is restricted to the medial rectus and lateral rectus muscles as actuators, and they were modeled using Hill's equations [12]. The eye is modeled as a solid sphere with rotational inertia J_G , rotational viscosity B_G and linear spring constant K_G around a vertical axis through its center. It is assumed that the medial rectus and lateral rectus muscles have identical characteristics, each having a mass M . A schematic model is presented in Figure 1.

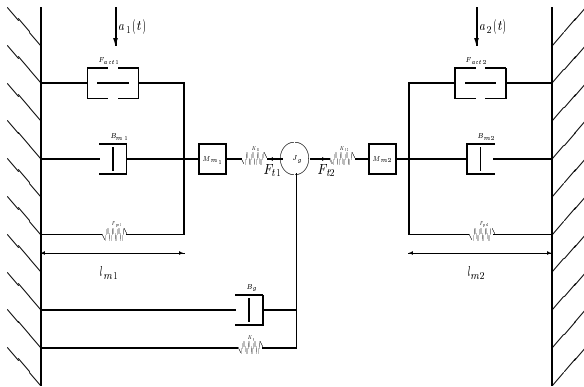


Figure 1: Oculomotor Plant

In [2], dynamical equations were derived to repre-

sent the model depicted in Figure 2.1, consisting of twelve coupled nonlinear differential equations with two neural control inputs. It was shown that a reasonably good approximation consisting of eight state variables can be derived in the form,

$$\dot{x} = f(x) + g_1(x)n_1(t) + g_2(x)n_2(t) \quad (1)$$

where, x represent the state vector, f, g_1 and g_2 are nonlinear vector fields to be described later, and n_1 and n_2 represent the neural input signals to the medial rectus and lateral rectus muscles, respectively. The state vector of the oculomotor plant is $x = [\theta, \dot{\theta}, F_{t1}, F_{t2}, l_{m1}, l_{m2}, a_1, a_2]'$ where,

θ	=	eyeangle
$\dot{\theta}$	=	angular velocity of the eye
F_{t1}	=	tendon force of the medial rectus muscle
F_{t2}	=	tendon force of the lateral rectus muscle
l_{m1}	=	length of the medial rectus muscle
l_{m2}	=	length of the lateral rectus muscle
a_1	=	activation level of the medial rectus muscle
a_2	=	activation level of the lateral rectus muscle.

Of course, the state space is a proper subset of \mathbb{R}^8 since several of the state variables have to satisfy hard constraints. For the sake of simplicity, only the following constraints are imposed here.

- Tendon forces are not allowed to fall below a minimum threshold level or exceed a maximum threshold level.
- Muscle lengths have to be between a lower and an upper limit.
- Neural activation levels of the medial rectus and lateral rectus muscles have to be between 0 and 1.

Below we describe the vector fields f, g_1 , and g_2 :

$$f(x) = \begin{bmatrix} x_2 \\ (x_3 - x_4 - B_g x_2 - K_g x_1) / J_g \\ K_t(x_3)[-x_2 - (180/\pi)\phi(x_3, x_5, x_7)] \\ K_t(x_4)[x_2 - (180/\pi)\phi(x_4, x_6, x_8)] \\ \phi(x_3, x_5, x_7) \\ \phi(x_4, x_6, x_8) \\ -x_7/\tau \\ -x_8/\tau \end{bmatrix} \quad (2)$$

$$g_1(x) = \frac{1}{\tau}[0, \dots, 0, 1, 0]'$$

$$g_2(x) = \frac{1}{\tau}[0, \dots, 0, 1]'$$

Here, τ represent a time constant reflecting the delay in converting neural signals to muscle activation signals, and K_t and ϕ are nonlinear functions,

$$K_t(x) = \begin{cases} k_{te}x + k_{tl}; & 0 \leq x \leq F_{tc} \\ k_s; & x \geq F_{tc}, \end{cases} \quad (3)$$

$$\phi(x, y, z, w) = \begin{cases} V_{max} \left[\frac{x - F_{pe}(y)}{z F_{max} F_l(y)} - 1 \right]^3; & z \geq c \\ \frac{-K_t(x)z}{\psi(y) + (180/\pi r)K_t(x)}; & z < c. \end{cases} \quad (4)$$

The function parameters F_{pe} , F_l and ψ in the expressions of ϕ are given by,

$$\psi(l) = \begin{cases} \frac{k_{mi}}{k_{me}} [exp(k_{me}(180/\pi r)(l - l_{ms}); \\ \quad \text{if } l_{ms} \leq l \leq l_{mc}, \\ (180/\pi r)k_{pm}; \quad \text{if } l \geq l_{mc}, \\ 0; \quad \text{otherwise,} \end{cases}$$

$$F_{pe}(l) = \begin{cases} \frac{k_{mi}}{k_{me}} [exp(k_{me}(180/\pi r)(l - l_{ms}); \\ \quad \text{if } l_{ms} \leq l \leq l_{mc}, \\ k_{pm}(180/\pi r)(l - l_{mc}) + F_{mc}; \\ \quad \text{if } l \geq l_{mc}, \\ 0; \quad \text{otherwise,} \end{cases}$$

$$F_l(l) = 1 - \left(\frac{l/l_{opt} - 1}{w} \right)^2.$$

Approximate values of the constants appearing in the functions above were estimated in [2] to be:

3 Control Design Methodology

The system described above is organized in a hierarchy similar to the treatment in backstepping. It turns out that strict backstepping isn't possible with this model, but the bothersome terms can be treated using the theory of singular perturbations.

Here the problem of the eye tracking signal $\theta_r(t)$ is discussed where no assumptions are made regarding the details of the dynamics of $\theta_r(t)$. The only assumption made is that at time t the brain is aware of the value of θ_r and its first three derivatives. A physical example that would fit this description would be the motion of a fly. It is assumed that the head is at rest at all times. The aim is to generate representative neural signals that will ensure that the eye angle $\theta(t)$ will track the reference signal $\theta_r(t)$ asymptotically. Let us rewrite the dynamics of the first two equations in (1) as

$$\begin{aligned} \dot{x}_1 &= x_2, \\ \dot{x}_2 &= -\frac{K_g}{J_g}x_1 - \frac{B_g}{J_g}x_2 + \frac{1}{J_g}(x_3 - x_4) \end{aligned} \quad (5)$$

parameter	description	value
r	radius of the eye	1.24cm
J_g	rotational inertia of the eye	6×10^{-5} $gts^2/0$
B_g	rotational viscosity of the eye	0.0158 $gts/0$
K_g	rotational viscosity of the eye	0.79gt/0
B_{pm}	passive muscle viscosity	0.06gts/0
M	muscle mass	0.748g
F_{max}	max. isom. mus. force	100gt
l_{mp}	primary muscle length	4.0cm
l_{opt}	optimal muscle length	4.65cm
l_{ms}	muscle slack length	3.7cm
l_{mc}	linear limit of passive muscle	4.8cm
k_{me}	a shape parameter	0.0387/0
k_{pm}	linear passive muscle elasticity	0.9gt/0
k_{ml}	min. pas. mus. elasticity	0.126gt/0
F_{mc}	linear limit of muscle force	20gt
w	a normalizing parameter	0.5
V_{max}	maximum muscle velocity	5689 ⁰ /s
k_s	linear tendon elasticity	2.5gt/0
k_{tl}	minimum tendon elasticity	1.5gt/0
k_{te}	a shape parameter	0.0333/0
l_{ts}	tendon slack length	0.2cm
l_{tc}	a shape parameter	0.532cm
F_{tc}	a shape parameter	30gt

Table 1: Parameters and estimated values

where $x_1 = \theta$, $x_2 = \dot{\theta}$, x_3 and x_4 are the tendon forces of the medial and lateral rectus muscles. The aim here is to ensure that $x_1(t) - \theta_r(t) \rightarrow 0$ exponentially fast.

Let us temporarily treat $(x_3 - x_4)$ as a control input $v(t)$ to 5, so that it has the appearance of a second-order linear control system. It is also stable since its eigenvalues are at -51.0, -3109.0 corresponding to the assumed values of J_g , K_g and B_g . (These figures suggest a fairly high amount of damping and stiffness, and physiological reasons behind them are not clear from the literature) Therefore, the tracking problem can be solved if one were to take

$$v(t) = K_g\theta_r + B_g\dot{\theta}_r + J_g\ddot{\theta}_r, \quad (6)$$

for in this case, if the tracking error is defined as

$$(e_1, e_2) = (x_1 - \theta_r, x_2 - \dot{\theta}_r), \quad (7)$$

then the error dynamics satisfy

$$\dot{e}_1 = e_2 \quad (8)$$

$$\dot{e}_2 = \frac{180}{J_g}e_1 - \frac{g}{J_g}e_2, \quad (9)$$

and this system has eigenvalues at $(-51.0, -3109.0)$.

Note that the third and fourth equations of (1) are,

$$\begin{aligned} \dot{x}_3 &= K_t(x_3)[-x_2 - (\frac{180}{\pi r})\dot{l}_{m_1}] \\ \dot{x}_4 &= K_t(x_4)[x_2 - \frac{180}{\pi r}\dot{l}_{m_2}]. \end{aligned} \quad (10)$$

Since the function $K_t(\cdot)$ is bounded from below, (10) can be solved for \dot{l}_{m_1} and \dot{l}_{m_2} for any desired expression for \dot{x}_3 and \dot{x}_4 . The strategy here is as follows. As it was argued earlier, $(x_3(t) - x_4(t))$ is needed to be controlled so that it will converge to the right hand side of (6) fast. This can be achieved by letting,

$$\dot{x}_3 - \dot{x}_4 = -\alpha(x_3 - x_4) + \dot{v}(t) + \alpha v(t), \quad (11)$$

where, α is a sufficiently large positive constant (α is chosen to be equal to 10 in the simulations to follow), and $v(t)$ is given in (6).

Define,

$$\begin{aligned} \gamma(t) &= \dot{v}(t) - \alpha v(t) \\ &= J_g \frac{d^3}{dt^3}\theta_r(t) + (B_g + \alpha J_g) \frac{d^2}{dt^2}\theta_r(t) + \\ &\quad (K_g + \alpha B_g) \frac{d}{dt}\theta_r(t) + \alpha K_g \theta_r(t). \end{aligned} \quad (12)$$

Here the aim is to choose \dot{l}_{m_1} and \dot{l}_{m_2} such that the difference in the right hand sides of (10) is equal to the right hand side of (11). Solutions to this problem are clearly non-unique. This non-uniqueness has to be exploited to find physiologically realistic solutions. The relevant physiological constraints translate to the following:

1. muscle activations are in the range $[0, 1]$.
2. for small values of muscle activation the equation (10) cannot be inverted to solve for \dot{l}_{m_i} .

Additionally, physiological evidence has been reported to point out that the tendon forces never fall below a certain minimum value.

In view of the above an arbitrary minimum value for the muscle tendon forces is fixed here (set at 10 gt in the simulations to follow). This bound is imposed indirectly via (10) by setting,

$$\begin{aligned} \dot{x}_3 &= -\alpha x_3 + \gamma_1(t) \\ \dot{x}_4 &= -\alpha x_4 + \gamma_2(t), \end{aligned} \quad (14)$$

where γ_1 and γ_2 are always kept above α times the minimum tendon force. Due to the high bandwidth of (14) this ensures that $x_3(t)$ and $x_4(t)$ will seldom fall below the desired minimum value.

Let F_{min} = minimum muscle tendon force allowed. Now, the following limitations on γ_1 and γ_2 are imposed:

- a) $\gamma_i(t) \geq (\alpha F_{min})$, $i = 1, 2$,
- b) $\gamma_1(t) - \gamma_2(t) = \gamma(t)$, where $\gamma(t)$ is given in (13).

To meet these requirements choose $\gamma_i(t)$ as,

$$\gamma_1(t) = \begin{cases} \alpha F_{min} + \gamma(t), & \text{if } \gamma(t) \geq 0 \\ \alpha F_{min}, & \text{if } \gamma(t) < 0. \end{cases} \quad (15)$$

$$\gamma_2(t) = \begin{cases} \alpha F_{min}, & \text{if } \gamma(t) \geq 0 \\ \alpha F_{min} - \gamma(t), & \text{if } \gamma(t) < 0. \end{cases} \quad (16)$$

Finally, from (10) and (14), it follows that,

$$\dot{l}_{m_1} = \left\{ \frac{1}{K_t(x_3)} [\alpha x_3 - \gamma_1(t)] - x_2 \right\} \frac{\pi r}{180} \quad (17)$$

$$\dot{l}_{m_2} = \left\{ \frac{1}{K_t(x_4)} [\alpha x_4 - \gamma_2(t)] + x_2 \right\} \frac{\pi r}{180}, \quad (18)$$

where $\gamma_1(t)$ and $\gamma_2(t)$ are as in (15), $\gamma(t)$ is as in (13), and α is a reasonably large positive constant (chosen to be equal to 10 in the simulations).

Now, the muscle activations $a_1(t)$ and $a_2(t)$ are found by inverting (1). Of course these inversions will be valid only if the activations will fall in the range $[0, 1]$. Activations falling outside of the range will indicate either the attempted eye movement

fall outside the physiologically reasonable range, or that the feedback solution found here is inferior to the one employed physiologically. Simulations below illustrate that as long as the attempted eye movement is reasonable the proposed feedback law meet physiological constraints.

Assuming that the constraints are met, the muscle activations can be presented as,

$$\begin{aligned} a_1(t) &= \frac{x_3(t) - F_{pe}(l_{m_1}(t))}{F_{max}F_l(l_{m_1}(t))[1 + (\frac{\dot{l}_{m_1}(t)}{V_{max}})^{1/3}]}, \\ a_2(t) &= \frac{x_4(t) - F_{pe}(l_{m_2}(t))}{F_{max}F_l(l_{m_2}(t))[1 + (\frac{\dot{l}_{m_2}(t)}{V_{max}})^{1/3}]}, \end{aligned} \quad (19)$$

where, $\dot{l}_{m_1}(t)$ and $l_{m_2}(t)$ are given in (18).

Observe that (19) describe muscle activation as a state feedback control law. It utilizes the first three derivatives of the reference signal. The neural inputs can be computed as,

$$n_i(t) = a_i(t) + \tau \dot{a}_i(t), \quad i = 1, 2. \quad (20)$$

This completes the process of computing representative neural signals to the medial rectus and lateral rectus muscles during the pursuit of the reference signal $\theta_r(t)$.

4 Some Simulation Results

Figures 2. and 3. display the tracking performance of the designed controller when the eye is tracking a sinusoidal signal (Figure 2.) and a ramp signal (Figure 3.).

References

[1] A. T. Bahill and B. T. Troost. Types of saccadic eye movements. *Neurology*, 29:1150–1152, 1979.

[2] A. McSpadden. A 2d dynamic model of human eye movement. Master’s thesis, Texas Tech University, Lubbock, Texas, 1998.

[3] M. Egerstedt. A model of the combined planar motion of the human eye. Master’s thesis, Royal Institute of Technology, Stockholm, Sweden, 1996.

[4] R. Robleto. An analysis of the musculotendon dynamics of hill-based models. Master’s thesis, Texas Tech University, Lubbock, Texas, 1997.

[5] P. Cooke. *A Dynamic 3D Model of the Human Eye Movement*. PhD Dissertation, Texas Tech University, 1998.

[6] R. H. Specter and B. T. Troost. The oculomotor system. *Ann. Neurol.*, 5:517–525, 1981.

[7] S. Squatrito and M. G. Maioli. Encoding of smooth pursuit direction and eye position by neurons of area mstd of macaque monkey. *The Journal of Neuroscience*, 17:3847–3860, 1997.

[8] B. T. Troost. Introduction to human eye movement control (web page) . <http://www.toddtroost.com/lectures/eyemove/elec.html>.

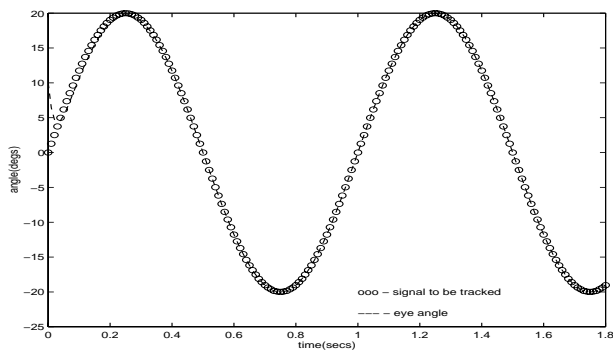
[9] B. T. Troost. An overview of oculomotor neurophysiology. *Ann. Otol. Rhinol. Laryngol.*, 4 part 3 suppl 86:29–36, 1981.

[10] B. T. Troost, R. B. Neber, and R. B. Daroff. Hemispheric control of eye movements, i: Quantitative analysis of refixation of saccades in a hemispherectomy patient. *Arch. Neurol.*, 27:449–452, 1972.

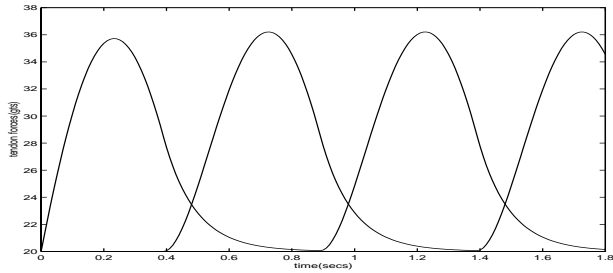
[11] B. T. Troost, R. B. Neber, and R. B. Daroff. Hemispheric control of eye movements, ii: Quantitative analysis of smooth pursuit in a hemispherectomy patient. *Arch. Neurol.*, 27:442–448, 1972.

[12] F. E. Zajac and W. S. Levine. Neuromuscular and musculoskeletal control models for the human leg. *Proc. 1983 ACC*, pp. 229–234, June 1983.

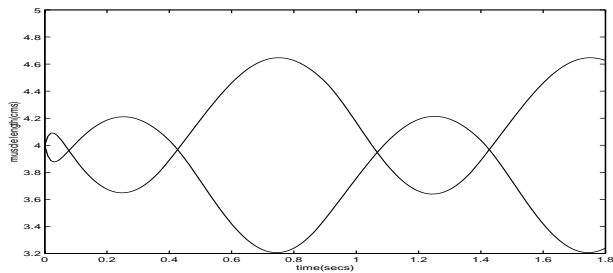
(a) Angles



(b) Tendon Forces



(c) Muscle Lengths



(d) Activation Forces

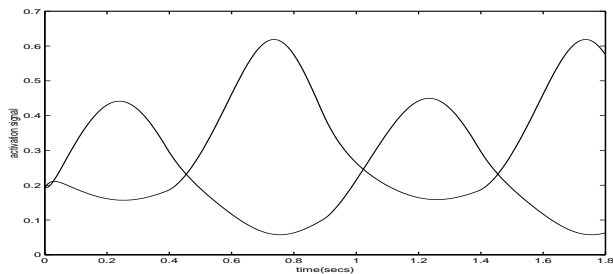
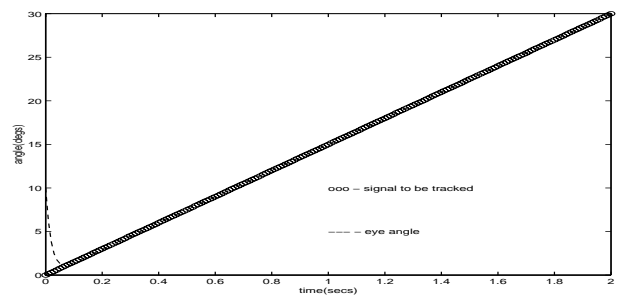
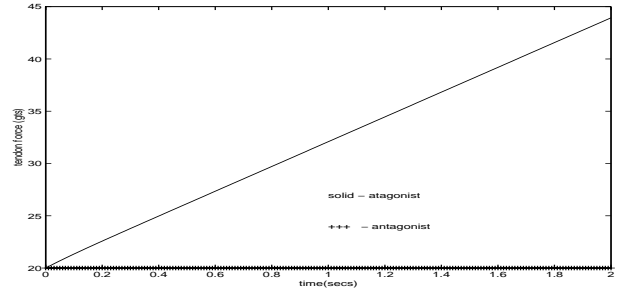


Figure 2: Tracking a sinusoidal signal $\theta_r(t) = 20.0 \sin(2\pi t)$

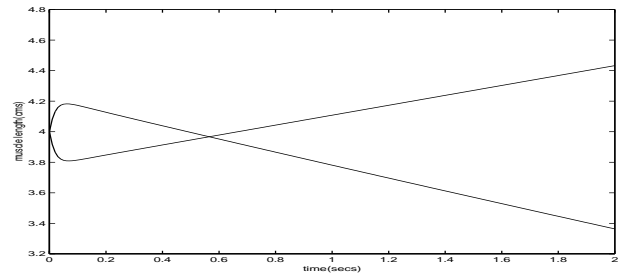
(a) Angles



(b) Tendon Forces



(c) Muscle Lengths



(d) Activation Forces

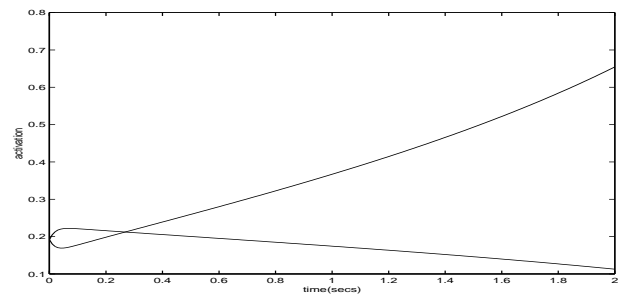


Figure 3: Tracking a ramp signal $\theta_r(t) = 15t$